

# Improvement of Nafion®-sepiolite composite membranes for PEMFC with sulfo-fluorinated sepiolite.

Christian Beauger, Guillaume Lainé, Alain Burr, Aurélie Taguet, Belkacem Otazaghine

▶ **To cite this version:**

Christian Beauger, Guillaume Lainé, Alain Burr, Aurélie Taguet, Belkacem Otazaghine. Improvement of Nafion®-sepiolite composite membranes for PEMFC with sulfo-fluorinated sepiolite.. Journal of Membrane Science, 2015, 495, pp.392-403. 10.1016/j.memsci.2015.08.014 . hal-01186135

**HAL Id: hal-01186135**

**https://minesparis-psl.hal.science/hal-01186135**

Submitted on 12 Jan 2021

**HAL** is a multi-disciplinary open access archive for the deposit and dissemination of scientific research documents, whether they are published or not. The documents may come from teaching and research institutions in France or abroad, or from public or private research centers.

L'archive ouverte pluridisciplinaire **HAL**, est destinée au dépôt et à la diffusion de documents scientifiques de niveau recherche, publiés ou non, émanant des établissements d'enseignement et de recherche français ou étrangers, des laboratoires publics ou privés.

# Improvement of Nafion®-sepiolite composite membranes for PEMFC with sulfo-fluorinated sepiolite

Christian Beauger [a,*], Guillaume Lainé [a], Alain Burr [b], Aurélie Taguet [c], Belkacem Otazaghine [c]

[a] MINES ParisTech, PSL Research University, PERSEE-Centre procédés, énergies renouvelables et systèmes énergétiques, rue Claude Daunesse, CS 10207, 06904 Sophia Antipolis Cedex, France

[b] MINES ParisTech, PSL Research University, CEMEF-Centre de Mise en Forme des Matériaux-UMR CNRS 7635, rue Claude Daunesse, CS 10207, 06904 Sophia Antipolis Cedex, France

[c] Centre des Matériaux C2MA, Ecole des Mines d'Alès, 6 avenue de Clavières, F-30319 Alès Cedex, France

A B S T R A C T

A new composite membrane based on Nafion® loaded with sulfo-fluorinated sepiolite was prepared, characterized and tested in a membrane electrode assembly in fuel cell operating conditions.

Pristine sepiolite, a natural microfibrous and highly hygroscopic clay, was first modified so as to make it proton conductive on one hand and to increase compatibility with Nafion® on the other hand. The proton conductivity was ensured through sulfonic acid groups while compatibility with Nafion® through fluorination of the grafted group. The functionalization was characterized with titration, thermal ana-lysis, pyrolysis-GCMS, FTIR and NMR. A mean graft concentration equivalent to 0.08 mmol/g was cal-culated which in this case also equals the ion exchange capacity of the modified sepiolite.

The composite membrane showed improved mechanical resistance (elastic modulus doubled for 10 wt% added sepiolite), unchanged IEC and larger water uptake compared to pure Nafion® membrane. The mechanical resistance was even better than that of our composite membrane previously prepared with sulfonated only sepiolite, most probably due to fluorination.

MEA performances were also significantly improved, especially at 100 °C and low RH (+50% more output power at 0.6 V at 50%RH).

*Keywords:*
Fuel cell
Membrane
Nafion
Composite
Sepiolite

## 1. Introduction

Proton Exchange Membrane Fuel Cells (PEMFC) are very promising electrochemical converters able to provide heat and electricity from Oxygen and Hydrogen. They are already widely tested for stationary, mobile and transport applications. However they still face some limitations related to their restricted temperature range of utilization. Such a limitation is due to the nature of the membrane, based on Nafion®, used as the electrolyte is these electrochemical converters. A lot of different works have already been focussed on looking for alternatives allowing to increase PEMFC operating temperature.

Numerous different fillers have been tested for years to modify the properties of Nafion® membranes and make them more thermomechanically resistant at intermediate temperature, less permeable or less sensitive to relative humidity. These modifications of properties are asked for various purposes. Increasing the operating temperature of proton exchange membrane fuel cells would provide numerous benefits regarding the cathode reaction kinetics, the pollutant tolerance (especially that of CO), heat, gas and water management or the choice of catalyst [1,2].

Alternative polymers have been evaluated for years for intermediate operating temperature. Phosphoric acid doped polybenzimidazole ($H_3PO_4$–PBI) is among most promising ones at high temperature [3–5]. Crosslinking with various polymers for an improved mechanical resistance [6–8] and block copolymers for improved proton conductivity without any humidification [9,10] have been recently reported. Sulfonated polyether(ether)ketones, polyimides or poly(ether)sulfones are still under investigation [11]. More recently, short side chain (SSC) perfluorinated sulfonic acid (PFSA) based membranes have shown good performance at intermediate temperature [12,13] due to higher crystallinity compared to long side chain (LSC) ionomers [14,15]. To date, Nafion® remains however the polymer of choice for proton exchange membrane fuel cells. Yet it is not really adapted to operating

* Corresponding author: Fax: +33 4 93 95 75 35.
*E-mail address:* christian.beauger@mines-paristech.fr (C. Beauger).

temperatures higher than 90 °C whereas its use would decrease many constraints on the quality of hydrogen or the system cooling for instance.

Metal oxides such as $SiO_2$ [16–23], $ZrO_2$ [24,25] or $TiO_2$ [26–32] have been used to simultaneously decrease the membrane hydrogen crossover and its sensitivity to relative humidity, without significantly impacting the membrane proton conductivity below roughly 10 wt% loading. Acids [33–38], phosphates or phosphonates [39–42] have the additional advantage to increase the membrane ion exchange capacity with beneficial effect on its proton conductivity. Clays, pristine or modified, have also been evaluated as promising fillers for different polymer matrices. Smectite clays like natural montmorillonite [43–48] or synthetic laponite [49–53] have received much attention for their barrier properties. Fibrous ones, palygorskite [54,55] or sepiolite [56–59], have been less studied.

Sepiolite is particularly interesting because of its fibrous morphology. We have shown that sepiolite can increase the mechanical properties of Nafion® membrane while significantly decreasing its sensitivity to relative humidity, especially at intermediate temperature [59]. Once functionalized to make it proton conductive, it allows improving fuel cells performance at 100 °C.

Controlling the dispersion of nanoparticles into polymer matrices is a significant challenge in achieving the properties improvements of nanocomposites. However, it is a priori difficult to achieve this objective as inorganic fillers are typically hardly compatible with polymers due to a poor affinity [60,61]. A variety of methods were developed to improve the affinity of particles toward a polymer with the introduction of molecules or macromolecules on fillers surface. These methods of surface modification include physical adsorption [62,63] and covalent binding at the surface of the particle [64].

Among the covalent binding which is undoubtedly the most used and performing method, different kind of functionalization can be distinguished. Silane coupling agents are classically used to functionalize silica nanoparticles [65–67], siliceous fillers [68] and metal oxides (aluminum, zirconium, tin, titanium, and nickel). These compounds allow a direct introduction of an organic group to the surface of mineral fillers. Silane coupling agents can also be used for more complex surface modifications. Indeed, they are now more commonly used to introduce polymer chains at the surface of nanoparticles. Grafting of polymer chains at the surface of nanoparticles is another route for promoting uniform nanoparticle dispersion and for generating nanocomposites with homogeneous properties. Different methods were developed including grafting from, grafting onto and grafting through strategies. Until now, the most commonly used polymers are homopolymers and especially PS and PMMA [69,70].

In this work, we have added another functionality to sepiolite to make it more compatible with Nafion®. To this end a fluorinated alkyl group has been added during the functionalization protocol to prepare a so-called sulfo-fluorinated sepiolite. This may improve phase nanosegregation in the membrane, interaction with Nafion® backbone and thus increase the membrane mechanical resistance and the overall performance.

Composite membranes have been prepared with 5, 10 and 20 wt% load of sepiolite functionalized with a new sulfo-fluorinated molecule. Membranes were characterized so as to evaluate their thermal and mechanical resistance, to calculate their ion exchange capacity, swelling, water uptake and proton conductivity.

A membrane electrodes assembly was finally prepared with 10 wt% of modified sepiolite and tested in fuel cell operating conditions, at 75 and 100 °C, between 25% and 100% relative humidity. Polarization curves, open circuit voltage, MEA resistance and hydrogen crossover were compared to those of our previous membranes prepared with pure Nafion® and Nafion® loaded with sulfonated only sepiolite.

## 2. Experimental

### 2.1. Raw materials

(3-glycidyloxypropyl)trimethoxysilane (GPTMS), sulfanilic acid (99% purity), perfluorooctanoic acid, 1,2-epoxydodecane (95% purity), methanesulfonic acid ( $\geq$ 99.5%), methanol (99% purity), toluene (99.8%) were purchased from Sigma Aldrich; NaOH ( $>$ 97% purity) and sulfuric acid (98% purity) were purchased from Prolabo; 0.5 M nitric acid was purchased from Riedel-de-Haën (69%); acetone (99.5% purity), chloroform (99.9% purity) and ethanol (96% purity) were purchased from Panreac; 5% hydrogen peroxide was purchased from Fluka (30%). All these products were used as received without any purification. Sepiolite Pangel S9 was provided by Tolsa (specific surface area: 320 $m^2/g$). This Pangel S9 sepiolite contains 85% of sepiolite and 15% of other clays.

### 2.2. Sepiolite functionnalization and characterization

Following our previous work, a new type of modified sepiolite has been used in this study. Compared to our former study, focussed on sepiolite sulfonation, the purpose was here to add a fluorinated side chain during functionalization in order to increase the compatibility of the modified sepiolite with Nafion®.

The functionalization of sepiolite was performed in several steps.

First, epoxy and $-SO_3Na$ groups were grafted according to the process described previously to prepare sulfonated sepiolite [59].

An additional procedure was then followed to add fluorinated groups on sulfonated sepiolite.

Into a 500 ml flask equipped with a Dean Stark apparatus were introduced 5 g of sulfonated sepiolite, 0.5 g ($1.2 \times 10^{-3}$ mol) of perfluorooctanoic acid, 300 ml of chloroform and 5 mg ($5 \times 10^{-5}$ mol) of methanesulfonic acid. The mixture was then stirred and heated at chloroform reflux for 15 h. The water formed during the reaction was eliminated by the Dean Stark apparatus. After reaction, the mixture was centrifuged (speed: 400 rpm) to eliminate the liquid phase and washed three times with acetone. The filler was dried under vacuum before characterization.

The whole process is described in Fig. 1, showing the structure of the so-called sulfo-fluorinated sepiolite (named hereafter SF-Sep).

This new modified sepiolite was fully characterized by titration (IEC), thermogravimetric analysis (TGA), FTIR and Pyrolysis coupled to Gas Chromatography and Mass Spectroscopy (Py–GCMS).

Titration has been carried out following a standard protocol. The fully protonated sepiolite was immersed, under $N_2$ atmosphere, overnight in 50 mL of 0.001 M NaOH (solution prepared from Acros organics pellets) and 0.1 M NaCl (Sigma Aldrich S3014) in order for the $Na^+$ ions to replace the $H^+$ of the sulfonated groups, which thus make the solution pH decrease. The remaining $HO^-$ ions were then titrated with 0.001 M HCl (prepared from 1 M HCl Fluka 84425), thus allowing to calculate the number of protons exchanged. The IEC is expressed as the number of millimoles of protons exchanged per gram of dry sepiolite (meq/g).

Thermal characterization was carried out by thermogravimetric analysis (Perkin Elmer Pyris-1 instrument) on 10 mg of samples, under nitrogen. Samples were first heated at 10 °C/min from 25 to 110 °C, followed by an isotherm at 110 °C for 10 min. They were then heated again from 110 to 900 °C, at 10 °C/min, in order to eliminate the grafted groups.

ATR-FTIR measurements (Bruker-IFS66) were carried out in the range of 4000–400 $cm^{-1}$, with 8 scans and spectral resolution of 1 $cm^{-1}$.

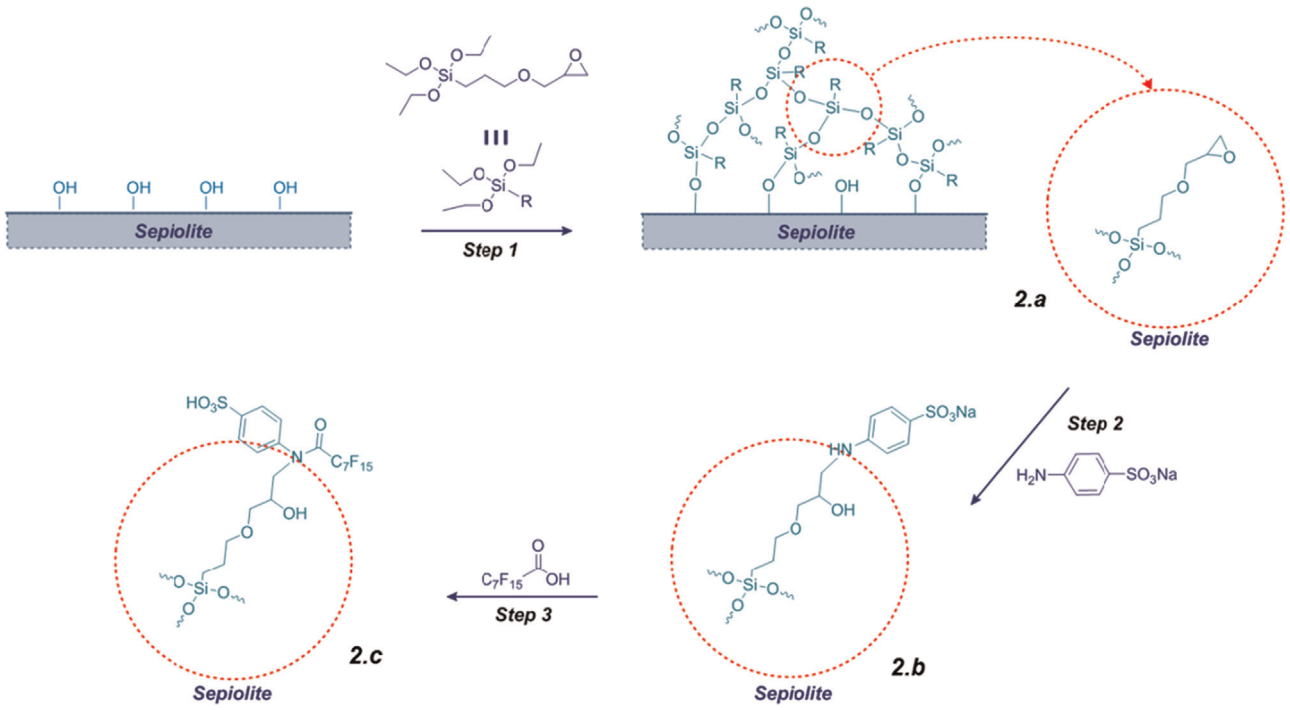



**Fig. 1.** Double functionalization of sepiolite to introduce $-SO_3H$ and $-C_7F_{15}$ groups.

The Py–GC/MS analytical setup consisted of an oven pyrolyzer connected to a GC/MS system. A Pyroprobe 5000 pyrolyzer (CDS Analytical) was used to pyrolyze the samples in a helium environment. This pyrolyzer is supplied with an electrically heating platinum filament. One coil probe enables the pyrolysis of samples (less than 1 mg) placed in quartz tube between two pieces of quartz wool. The sample was heated directly at 900 °C or successively heated at 200, 400, 600 and 900 °C. Each temperature was held for 15 s before gases were drawn to the gas chromatograph for 5 min. The pyrolysis interface was coupled to a 450-GC gas chromatograph (Varian) by means of a transfer line heated at 270 °C. In this oven the initial temperature of 70 °C was held for 0.2 min, and then raised to 250 °C at 10 °C/min. The column is a Varian Vf-5 ms capillary column (30 m × 0.25 mm) and helium (1 mL/min) was used as the carrier gas; a split ratio was set to 1:50. The gases were introduced from the GC transfer line to the ion trap analyzer of the 240-MS mass spectrometer (Varian) through the direct-coupled capillary column. Identification of the products was achieved comparing the observed mass spectra to those of the NIST mass spectral library.

NMR spectra were recorded on Bruker AC 400 instruments, using deuterated dimethyl sulfoxide as the solvent and tetramethylsilane as the references for 1H nuclei. Chemical shifts are given in part per million (ppm). The experimental conditions for recording $^1$H NMR spectra were as follows: flip angle 90°, acquisition time 4.5 s, pulse delay 2 s and number of scans 16.

### 2.3. Membrane and membrane electrodes assembly (MEA) preparation

The membranes (13 × 13 cm$^2$) were prepared by casting, following the protocol described in an earlier publication [59], starting from an Ion Power DE2021 Nafion® dispersion. The only difference stands in the type of sepiolite added in the dispersion. Here we have used our new modified sepiolite, a sulfo-fluorinated sepiolite. Membranes are named M112SxSF where *x* stands for the wt% of modified sepiolite.

MEAs were also prepared following the protocol described in the same paper [59], hot pressing the membranes between two commercial electrodes (Paxitech, 50 cm$^2$, 0.6 mg Pt/cm$^2$).

### 2.4. Membranes characterizations

Water uptake, swelling, Ion Exchange Capacity (IEC), thermogravimetric analysis (TGA), microscopies (SEM), dynamic mechanical analysis (DMA) and conductivity measurements have been performed to characterize the membranes.

#### 2.4.1. Water uptake

The water uptake ($W_{ut}$) was measured from the difference of the weight of a membrane stored in water at room temperature ($W_w$) and that of the same membrane dried out at 80 °C for 15 h ($W_d$), according to the following formula, $W_{ut} = (W_w - W_d)/W_d \times 100$.

#### 2.4.2. Swelling

In the presence of water, membranes tend to swell, leading to mechanical constraints in the fuel cell stack, all the more important as more MEAs are stacked. The swelling ($S_i$) was measured as the percentage of size increase in the direction i of the membrane ($i$=1 for side 1, 2 for side 2 and "th" for the thickness). These percentages were calculated by difference between the size measured after equilibration of the membrane in water at room temperature (RT) on one hand and boiling water (BT) on the other hand. Hence, $S_i$ the swelling percentage in the direction $i$ was calculated as followed: $S_i = 100 \times [(x_i)_{BT} - (x_i)_{RT}]/(x_i)_{RT}$, where $(x_i)_{BT}$ is the length of the membrane in the direction $i$ in boiling water and $(x_i)_{RT}$ is the length of the membrane in the direction i in water at room temperature. For the thickness swelling, we have $S_{th} = 100 \times (th_{BT} - th_{RT})/th_{RT}$, "th" being the thickness measured in μm.

#### 2.4.3. Ion exchange capacity (IEC)

The IEC was measured by titration according to the procedure described in 2.2. The fully protonated membrane was immersed overnight in 0.1 M NaOH (20 mL solution prepared from Acros

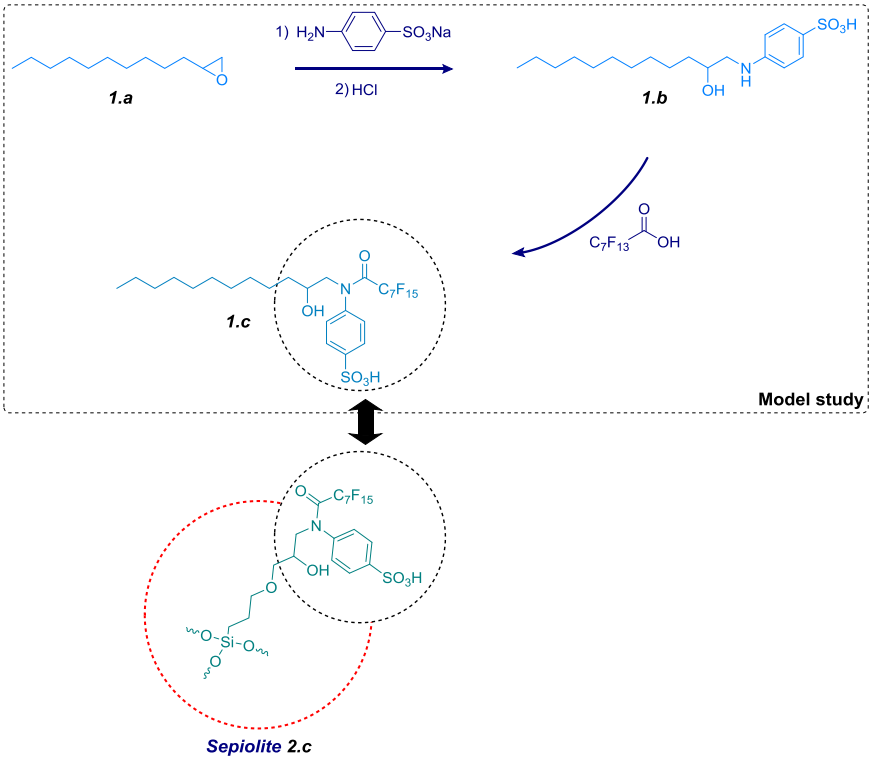



**Fig. 2.** Model study corresponding to the chosen procedure for double functionalization of sepiolite NFs.

organics pellets). The remaining $HO^-$ ions were titrated with 0.01 M HCl (prepared from 1 M HCl Fluka 84425).

#### 2.4.4. Thermogravimetric analysis (TGA)

Membranes were characterized by thermogravimetric analysis (Perkin Elmer Pyris-1 instrument) on 10 mg of samples, under nitrogen. Samples were heated at 10 °C/min from 25 to 900 °C.

#### 2.4.5. Microscopies (SEM, TEM)

Scanning Electron Microscopy (SEM) observations were realized on FEI XL30 ESEM equipped with a qualitative chemical analysis probe (EDS) to evaluate the sepiolite dispersion within the Nafion® matrix.

Transmission Electron Microscopy (TEM) observations were realized using a JEOL 1200 EXII.

#### 2.4.6. Mechanical tests

Mechanical tests were performed in order to control the influence of the fillers on the mechanical resistance of the membrane, which is closely related to its durability in FC operating conditions. Dynamic Mechanical Analysis, performed on a TRITEC 2000 in tensile mode, allowed to determine the Elastic modulus ($E$). The measurements were realised at 1 Hz and at a heating rate of 2 °C/min between 25 °C and 250 °C.

#### 2.4.7. Conductivity

The membrane conductivity was measured through plane by impedance spectroscopy (Biologic HCP 803). The membrane was first equilibrated in the cell at room temperature in the presence of liquid water in a reservoir to saturate the atmosphere with water vapor. The results presented here are mean values of measurements repeated three times with three different samples of each composition. The conductivity is calculated considering the high frequency resistance of the membrane, its thickness and the surface of the electrode.

### 2.5. MEAs characterization

50 $cm^2$ active surface area MEAs were tested on our Fuel Cell test bench, as already described earlier [71]. The polarization curves ($U=f(j)$) were performed at 75 and 100 °C and between 25 and 100% relative humidity (RH). The MEA resistance was measured by impedance spectroscopy. It was assimilated to the high frequency impedance value for its imaginary part equal to zero. According to Vielstich et al. [72] the membrane hydrogen crossover was measured in MEAs, applying a 0.5 V voltage at one electrode purged with Nitrogen while the other one is purged with Hydrogen. The Hydrogen crossing the membrane from the Hydrogen electrode to the Nitrogen one is oxidized, resulting in a current proportional to the Hydrogen flow across the membrane.

## 3. Results and discussion

### 3.1. Sepiolite characterization

To improve performance of Nafion® membranes used for PEMFC applications, a new strategy for sepiolite functionalization was developed. This strategy based on a multi-step reaction is presented in Fig. 1.

The first step is the sepiolite treatment by GPTMS to introduce an epoxy group. The second step is the introduction of a sodium sulfonate group by reaction between the epoxy group and the amine group of sodium 4-aminobenzenesulfonate. The epoxy group opening leads to the formation of a hydroxyl function and an aromatic secondary amine. These two kinds of group can react in a third step to introduce the perfluorinated group. Indeed the secondary amine or hydroxyl group can react with pentadecafluorooctanoic acid to form the corresponding amide or ester.

Our hypothesis of a preferential formation of the amide function was verified by a model study starting from 1,2-epoxydodecane, not grafted on sepiolite, to allow a simpler

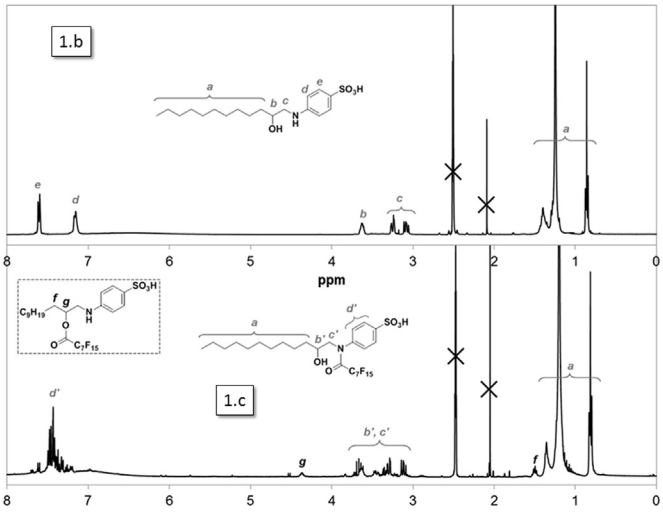



**Fig. 3.** $^{1}$H NMR spectra of products 1.*b* (up) and 1.*c* (bottom) recorded in d-DMSO.

characterization.

After validation by the model study, the double functionalization process was applied to sepiolite nanofibers (NFs) (Fig. 2).

### 3.1.1. Model study

A reaction between 1,2-epoxydodecane and sodium 4-aminobenzenesulfonate gives the corresponding β-amino alcohol. This first step corresponds to the introduction of the sodium sulfonate group in the fillers treatment procedure. Then, the compound obtained was reacted with perfluorooctanoic acid to introduce the fluorinated group.

Fig. 3 shows the $^{1}$H NMR spectra of the purified products 1.*b* and 1.*c* obtained respectively for both reactions. The NMR spectrum of product 1.*b* matches with the expected structure and proves the opening of the epoxide function and the formation of a hydroxyl and secondary amine group. The NMR spectrum of product 1.*c* shows differences for signals of aromatic protons compared to product 1.*b*. Two distinct doublets are observed at 7.2 and 7.6 ppm for 1.*b* and replaced by a very large multiplet between 7.2 and 7.7 ppm for 1.*c*. This corresponds to the tertiary amide formation by reaction of the secondary aromatic amine with the carboxylic acid. We can observe also an evolution of the signals between 3.2 and 3.6 ppm corresponding to the other protons near the nitrogen atom (protons b' and c' on the spectrum). However the appearance of two multiplets at 1.5 and 4.4 ppm, respectively (protons f and g on the spectrum), were attributed to the ester formation by reaction of the hydroxyl group with the carboxylic acid. The comparison of the intensity of the multiplet at 1.5 ppm (protons of $-CH_2-$ in $\alpha$ position of the ester on the alkyl chain) with the intensity of the triplet at 0.8 ppm ($-CH_3$ protons for both amide and ester products) gives a value of about 10% for the formation of the ester species.

The FTIR analyses (Fig. 4) also confirm the preferential formation of the amide species. Indeed the comparison between spectra of the products 1.*b* and 1.*c* shows the disappearance of two bands at 3385 and 1575 $cm^{-1}$ characteristic of the N–H bond of secondary amine and the appearance of a band at 1775 $cm^{-1}$ attributed to the C=O double bond of the amide species.

### 3.1.2. Sepiolite surface modification

In a first step the epoxide group was introduced on the surface filler. Afterwards, the same procedure as for the model study was applied. Thermogravimetric analyses were used to characterize the introduction of the sulfonic and fluorinated groups onto sepiolite surface (Fig. 5). Both fillers show an increase of the weight loss after each step of the modification procedure (Table 1). This tends to prove the efficiency of the procedure used. The silanol groups react with GPTMS in the first step to introduce the epoxide function. The calculation of the concentration of the grafted groups based on the weight loss shows very close values for sepiolite products 2.*b* and 2.*c* (0.068 and 0.064 mmol/g, respectively). This is a good indication that the reaction used to introduce the fluorinated group is quantitative.

The sulfonic acid group concentration has also been calculated with titration on sulfo-fluorinated sepiolite. The result (0.09 mmol/g) is consistent with that of TGA. The IEC of the modified sepiolite is one order of magnitude smaller than that of the Nafion® type which will be used to prepare the membrane. Hence we may expect a drop of the composite membrane ion exchange capacity.

Py–GC/MS was also used to evaluate the procedure of multifunctionalization of sepiolite NFs. Two kind of analyzes were used to characterize the different samples. The first one is a mono-pyrolysis at 900 °C to evaluate the presence and the nature of the organic molecules on the fillers surface. For the second one, sample 2.*c* was heated successively at 200, 400, 600 and 900 °C to evaluate the thermal stability of each part of the grafted molecule.

The results obtained for the mono-pyrolysis of sepiolite samples at 900 °C (Fig. 6) confirmed the TGA results. Chromatograms of the modified samples show peaks corresponding to organic molecules obtained by thermal degradation of the grafted part for both fillers. New peaks appear after each step of the chemical modification procedure. Sample 2.*b* shows the presence of molecules with nitrogen atom that were not evidenced for 2.*a*, attributed to the aromatic secondary amine on the surface fillers. Sample 2.*c* shows the presence of fluorinated molecules due to the introduction of the perfluorinated group during the last step. These results confirm the efficiency of the protocol used for sepiolite.

Concerning the multistep pyrolysis (200, 400, 600 and 900 °C), a GC/MS analysis was performed after each pyrolysis step to verify the nature of the molecules formed. All samples are stable at 200 °C and do not show any peak on their chromatograms. This absence of signals confirms a covalent anchoring of the organic part onto the fillers surface. Indeed this temperature is too low to induce cleavage of covalent bonds but high enough to allow desorption of free molecules. Pyrolysis at 400 °C shows the formation of molecules of degradation only for the product 2.*c* (Fig. 7) and absence of signals for the modified fillers 2.*a* and 2.*b* obtained for the first stages of the procedure. The signal observed for product 2.*c* at 400 °C appears at 1.8 min and is assigned to a fluorinated molecule containing $-C_7F_{15}$ groups. This large peak was attributed to the decomposition of the amide function which releases the perfluorinated group. This cleavage of the amide group is partial at 400 °C because other fluorinated molecules appear on the chromatograms when filler 2.*c* is pyrolyzed at 600 °C. All samples decompose at 600 °C and many peaks appear on their chromatograms. Chromatograms of samples 2.*b* and 2.*c* show the presence of nitrogen molecules which proves the decomposition of the amine group. The maximum release of containing nitrogen molecules is obtained for the last pyrolysis at 900 °C which confirms a good stability of the amine function. Chromatogram of product 2.*c* does not show fluorinated molecules for pyrolysis at 900 °C. This result confirms the lower thermal stability of the amide group.

### 3.2. Membrane preparation

Composite membranes were prepared with the newly modified sepiolite, with a targeted thickness of 50 μm. Their performance was compared to four reference membranes: a commercial Nafion® membrane labeled N112, a homemade Nafion® membrane,

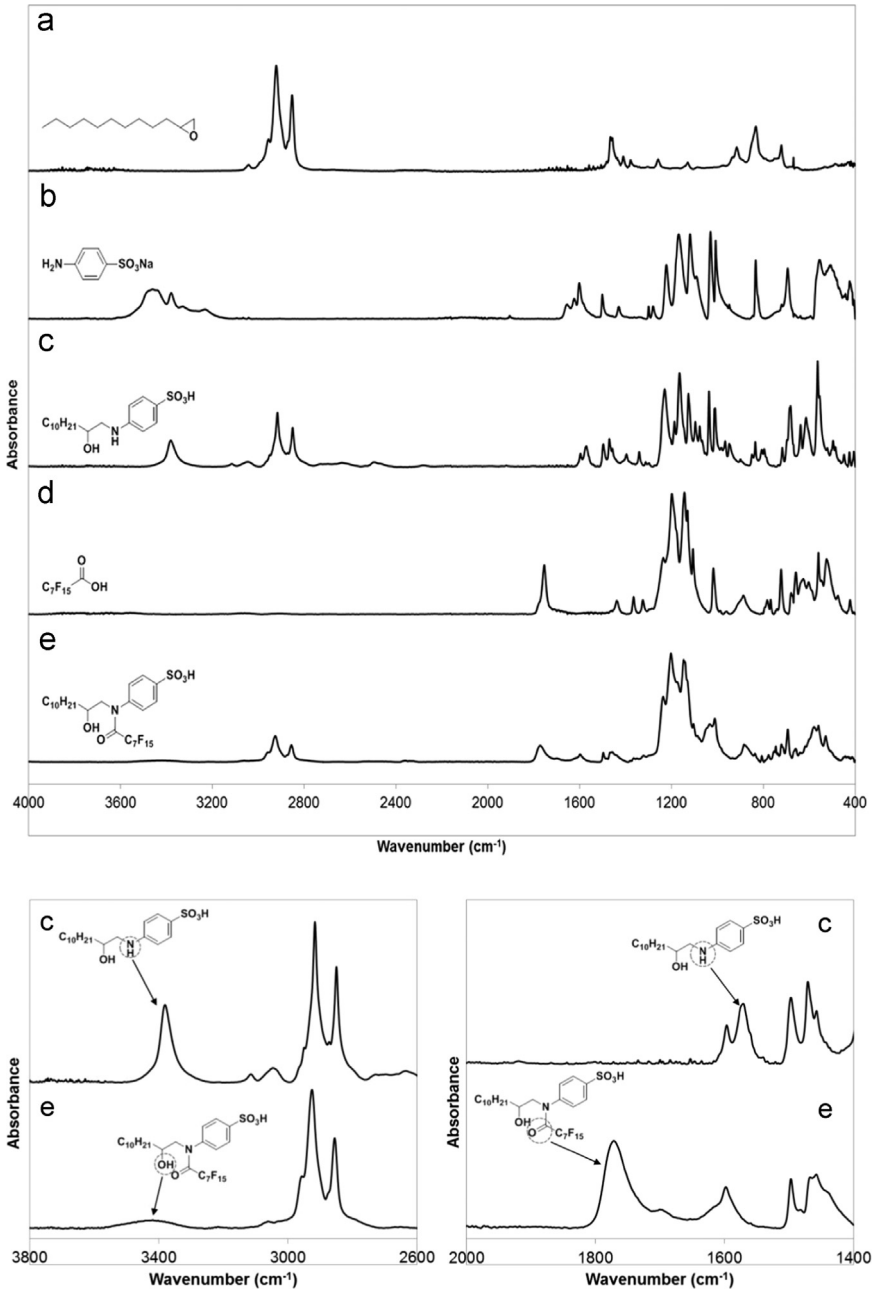



**Fig. 4.** ATR-FTIR spectra of 1,2-epoxydodecane (a), sodium 4-aminobenzenesulfonate (b), product 1.*b* (c), perfluorooctanoic acid (d) and product 1.*c* (e).

labeled M112 and two composite Nafion®-sulfonated sepiolite membranes, characterized previously, labeled M112S05SH and M112S10SH, the latter three prepared by casting.

Table 2 details the different membranes compared for this study.

### 3.3. Membrane characterization

The new composite membranes were first observed with SEM to check their global homogeneity. Looking at Fig. 8, no clear phase macro-segregation was evidenced between Nafion® and sulfo-fluorinated sepiolite throughout the thickness of the membranes loaded with 10 or 20 wt% modified sepiolite. Such a macro-segregation was indeed clearly visible with one of the modified sepiolite used in our previous work. It was confirmed by EDX measurements showing large excess of sepiolite on one side of the membrane. The new modified sepiolite used here does not entail such macroscopic inhomogeneity in the composite membrane. Whatever the SF-Sep concentration in the composite membranes prepared in the work presented here (10 or 20 wt%), EDX measurements showed similar amount of silicon throughout the membrane (Si/F = $0.004 \pm 0.001$ and $0.01 \pm 0.002$ respectively for M112S10SF and M112S20SF). TEM imaging (Fig. 9) reveals however the presence of aggregates of the size of a few microns.

The thermal behavior obtained for the pure and the composites membranes (Fig. 10) are almost identical to those described in the literature [25,73]. Three steps of weight loss were recorded, corresponding first to dehydration, then to desulfonation/defluorination and finally to decomposition of the polymer backbone. The sulfonic and fluoro-sulfonic groups grafted on sepiolite (M112S10SH and M11S10SF) start to decompose from 300 °C. At this same temperature desulfonation of the Nafion® membrane occurs. The weight loss at 300 °C is greater for composite membranes than for pure Nafion® membrane. This is probably due to

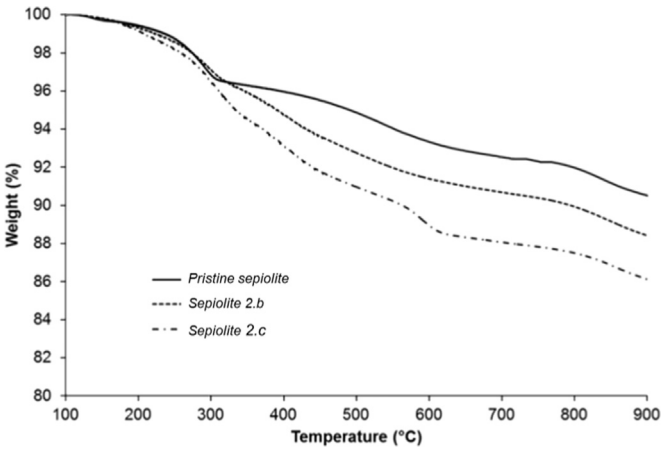



**Fig. 5.** TGA under nitrogen, from 100 °C to 900 °C and after an isotherm at 110 °C for 10 min, of pristine and modified sepiolite (2.*b*: sulfonated sepiolite, 2.*c*: sulfo-fluorinated sepiolite).

**Table 1**
TGA results used to calculate the concentration of $-SO_3H$ and $-C_7F_{15}$ at the surface of sepiolite.

| Sample | Weight loss due to the drying step (wt%) | Weight loss at 900 °C[a] (wt%) | Weight loss due to the grafting[a] (wt%) | Grafted group concentration (mmol/g) |
|---|---|---|---|---|
| **Pristine sepiolite** | 8.4 | 9.5 | – | – |
| **Sulfonated sepiolite (2.*b*)** | 4.1 | 11.6 | 2.11 | 0.068 |
| **Sulfo-fluorinated sepiolite (2.*c*)** | 3.2 | 13.9 | 4.41 | 0.064 |

[a] The weight loss refers to the sample after the drying step.

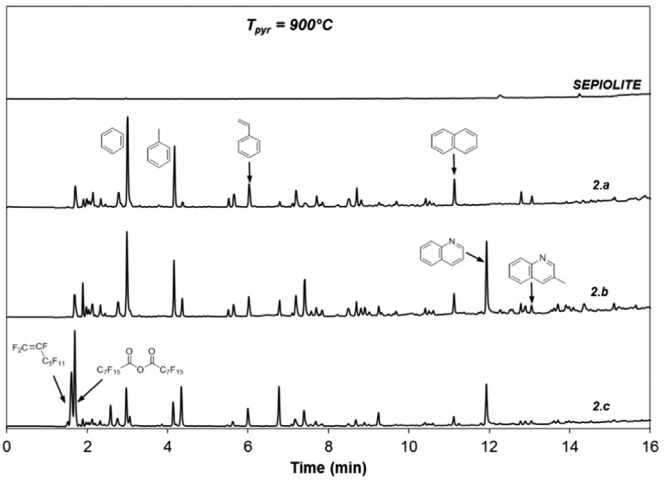



**Fig. 6.** Py–GC/MS chromatograms obtained for unmodified and modified sepiolite samples at 900 °C.

the elimination of grafted groups heavier than sulfonic groups resulting from the desulfonation of Nafion®.

The thickness, the ion exchange capacity, the water uptake and the swelling of the studied membranes are reported in Table 3. For comparison purposes, the features of previously studied membranes (N112, M112S05SH and M112S10SH) are also mentioned.

First of all, all the membranes have similar thickness, close to the targeted value of 50 μm. This parameter will thus not have to be taken into account when comparing the fuel cell performance.

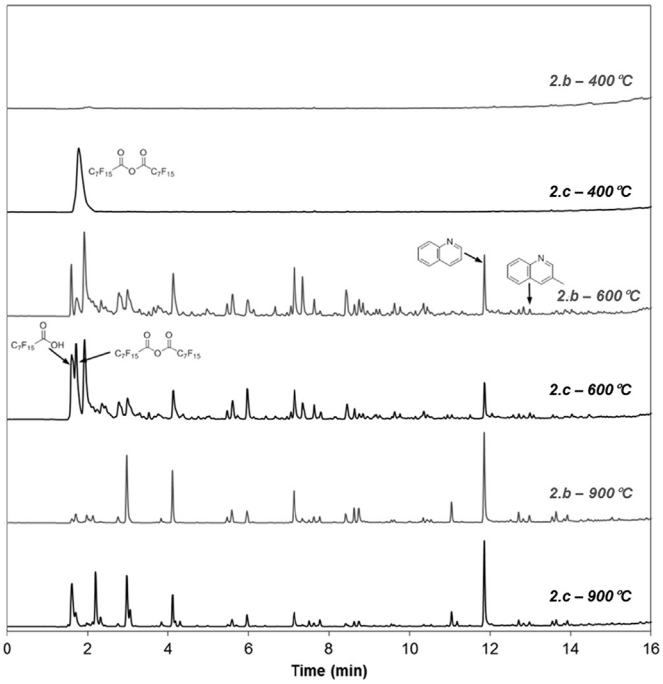



**Fig. 7.** Py–GC/MS chromatograms obtained for the sepiolite products 2.*b* and 2.*c*, pyrolyzed at 400, 600 and 900 °C.

**Table 2**
Membranes compared in the study.

| Membrane label | Sepiolite | |
|---|---|---|
| | Type | Amount (wt%) |
| N112 | – | 0 |
| M112 | – | 0 |
| M112SxSH | S-sepiolite | $x$=05, 10 |
| M112SxSF | SF-sepiolite | $x$=05, 10, 20 |

The introduction of modified sepiolite in the membrane does not make the composite membrane IEC significantly decrease, despite the quite low IEC measured for the modified sepiolite. Indeed we have already shown that introducing pristine sepiolite in a Nafion® membrane decreases its IEC, due to a dilution effect, whereas when sepiolite is sulfonated, the IEC is roughly kept unchanged. Here the sepiolite IEC is smaller than in our previous study without any influence on the composite membrane IEC. The fluorination performed on the sepiolite used for this study may have a beneficial effect on the nanophase segregation thus limiting the expected drop of IEC.

Considering both the water uptake and the swelling, the same trend as previously reported [59] is observed here: the higher the sepiolite content, the larger the water uptake and the swelling. This is in agreement with the known property of sepiolite to tremendously absorb water. Here again the thickness swelling is more pronounced.

The mechanical properties are of upmost importance as regards the durability of the membrane in an operating fuel cell. The elastic modulus of the different membranes has thus been measured by dynamics mechanical analysis and compared to that of our references (Fig. 11).

We have already shown that the introduction of sulfonated sepiolite in a Nafion® matrix allowed improving its mechanical resistance as evidenced by the increase of the elastic modulus reported on Fig. 11 (M112SxSH series). An even larger improvement has been obtained with SF-Sep as fillers. The elastic modulus

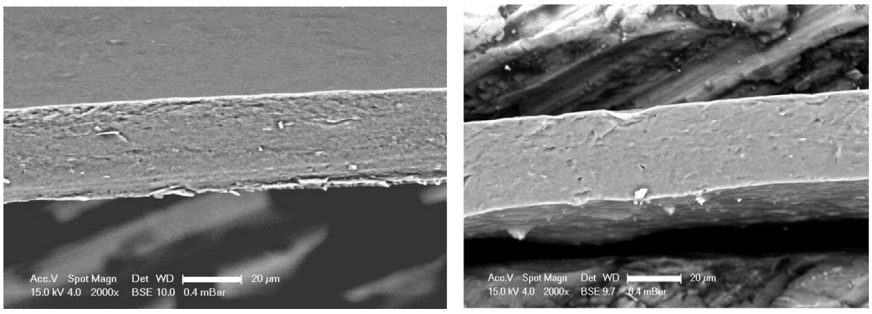



**Fig. 8.** SEM pictures of cryofractured composite membranes: M112S10SF (left) and M112S20SF (right).

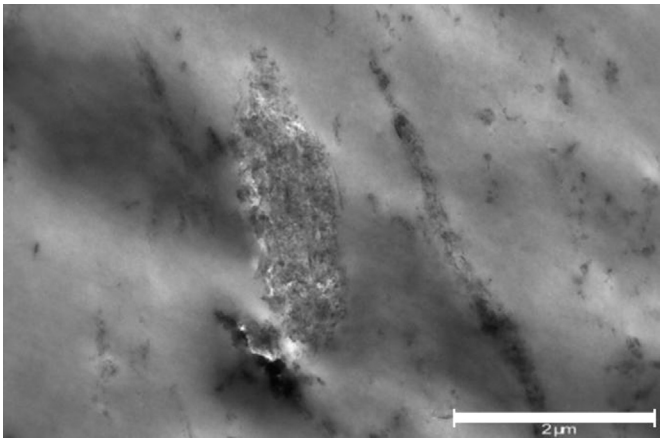



**Fig. 9.** TEM picture of M112S10SF showing some sepiolite aggregates.

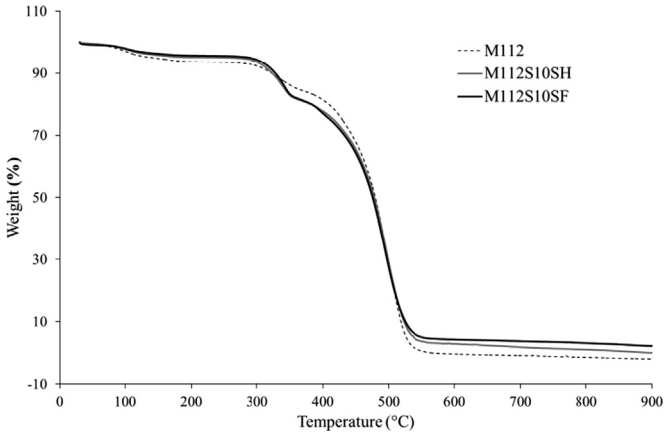



**Fig. 10.** TGA of pure Nafion® (M112) and composite with sulfonic and sulfofluorinated sepiolite (M112S10SH and M112S10SF, respectively).

**Table 3**
Membrane characterization results, (th = thickness, IEC = Ion Exchange Capacity, $W_{ut}$ = water uptake and $S$ = swelling).

| **Membrane** | **th** ± 1 (μm) | **IEC** ± 10% (meq/g) | $\boldsymbol{W_{ut}}$ ± 0.5 (wt%) | $\boldsymbol{S}$ ± 0.5 (%) | | |
|---|---|---|---|---|---|---|
| | | | | $s_1$ | $s_2$ | *th.* |
| N112 | 56 | 0.9 | 25 | 6 | 5 | 8 |
| M112 | 52 | 1.1 | 29 | 5 | 3 | 6 |
| M112S05SH | 44 | 1.2 | 34 | 5 | 5 | 7 |
| M112S05SF | 55 | 1.2 | 35 | 5 | 5 | 7 |
| M112S10SH | 48 | 1.2 | 38 | 6 | 6 | 10 |
| M112S10SF | *53* | 1.2 | *38* | 7 | 6 | 9 |
| M112S20SF | 49 | 1.1 | 42 | 7 | 7 | 12 |

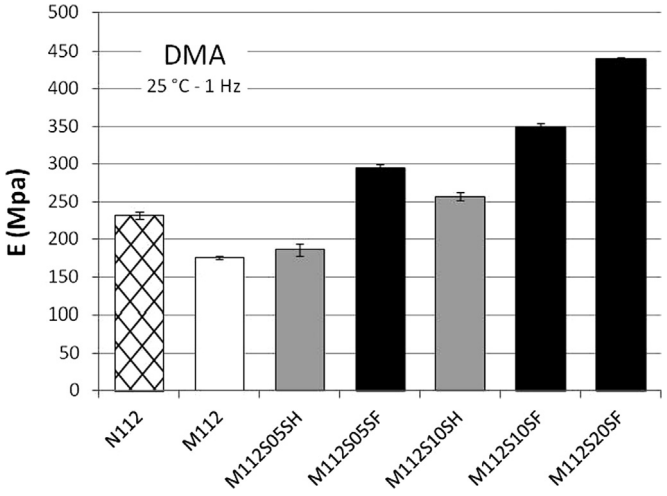



**Fig. 11.** Elastic modulus measured for the different membranes by Dynamics Mechanical Analysis at 25 °C and 1 Hz.

of the new composite membranes (M112SxSF series) is continuously increasing with the amount of SF-Sep in the range [5–20 wt%]. For 10 wt% it is almost doubled compared to that of M112, our pure Nafion® cast membrane. All the composite membranes prepared in this study present an elastic modulus even larger than that of the commercial Nafion® membrane N112 tested here. The fluorination of sepiolite allowed increasing significantly the mechanical resistance of the composite membranes, probably due to a better affinity with Nafion®. Indeed, the rather good dispersion of sepiolite is not the only reason for such an improvement. It may also most probably be ascribed to the dual nature of this newly modified sepiolite, hydrophobic and hydrophilic, such as Nafion® is. We suppose that, due to this dual nature, SF-Sep could interact with both the hydrophilic and the hydrophobic domains of Nafion®.

In comparison, we have characterized composite membranes prepared with fluorinated only sepiolite (not shown here). Their elastic modulus was unchanged compared to that of the pure Nafion® cast membrane. The interaction with the hydrophilic domains of Nafion® is essential to increase the mechanical properties of the composite, accounting for the improvement observed with both S-Sep (M112SxSH series) and SF-Sep (M112SxSF series).

The newly developed sepiolite (SF-Sep), sulfonated and fluorinated, allowed to prepare rather homogeneous composite membranes with Nafion®, presenting unchanged ion exchange capacity, larger water uptake and improved mechanical resistance (larger elastic modulus). These features, the latter presenting an improvement compared to sulfonated only sepiolite, should be beneficial to the use of these composite membranes as electrolytes in proton exchange membrane fuel cells.

The conductivity is another important feature. Since protons

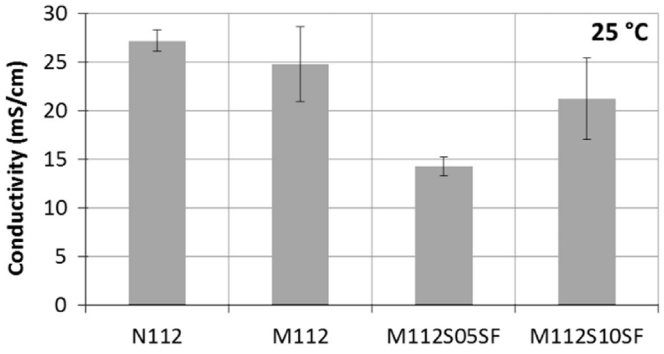



**Fig. 12.** Through plane conductivity of membranes, pure Nafion® (commercial N112 and recast M112) and composites with sulfo-fluorinated sepiolite (M112S05SF, M112S10SF).

are crossing the membrane during fuel cell operation, we preferred to measure through plane conductivity. The conductivity of composite membranes prepared with our newly modified sepiolite, i.e. the sulfo-fluorinated sepiolite, was calculated for 5 and 10 wt% loads and compared to that of pure Nafion® membranes, commercial N112 and homemade M112, obtained in the same conditions (Fig. 12).

The conductivity at 25 °C and 100%RH is similar for N112 and M112, close to 25 mS/cm.

Introducing sulfo-fluorinated sepiolite in Nafion® leads to a decrease in the conductivity . However, the higher the amount of modified sepiolite, the higher the conductivity. With 10 wt% of sulfo-fluorinated sepiolite, the conductivity is close to that of M112.

### 3.4. MEA single cell tests

We have compared the polarization curves of M112S10SF, obtained at 75 °C and 100 °C, between 25 and 75%RH, with those of M112 (Fig. 13) and M112S10SH (Fig. 14).

The polarization curves obtained at 75 °C are rather similar. If the performance of pure Nafion® are slightly better at 75%RH, performance of pure Nafion® and composite membrane M112S10SF are very similar at 50%RH (Cf Fig. 13). At 75 °C, the new composite membrane developed in this study gives slightly better performance than our previous composite membrane M112S10SH (Cf Fig. 14). 9% and 14% increase of current density were recorded respectively at 75%RH and 50%RH.

On the contrary, a very significant improvement was observed at 100 °C with the composite membrane prepared with SF-Sep compared to pure Nafion® membrane, whatever the relative humidity. Indeed, at 0.6 V, the current density measured for M112S10SF MEA is 25% higher than that of M112 MEA at 75%RH, 50% higher at 50%RH and even 130% higher at 25%RH (Cf Fig. 15).

The performance of the MEA prepared with M112S10SF are even slightly better than those of the MEA previously prepared with M112S10SH (4% and 15% increase of current density at 0.6 V, respectively at 50%RH and 25%RH).

Since the MEA resistance is responsible for ohmic losses and the hydrogen crossover impacts the open circuit voltage, it is often instructive to look at these features to analyze the polarization curves. They are reported on Fig. 16 for the different operating conditions chosen for the study.

Looking at Fig. 16a, the main parameter influencing the resistance is the relative humidity. As expected, the lower the relative humidity, the higher the resistance. The beneficial effect of composite membranes on the MEA resistance is observed only in severe conditions (100 °C, 25%RH). The decrease of resistance observed with M112S10SH is confirmed and even emphasized with

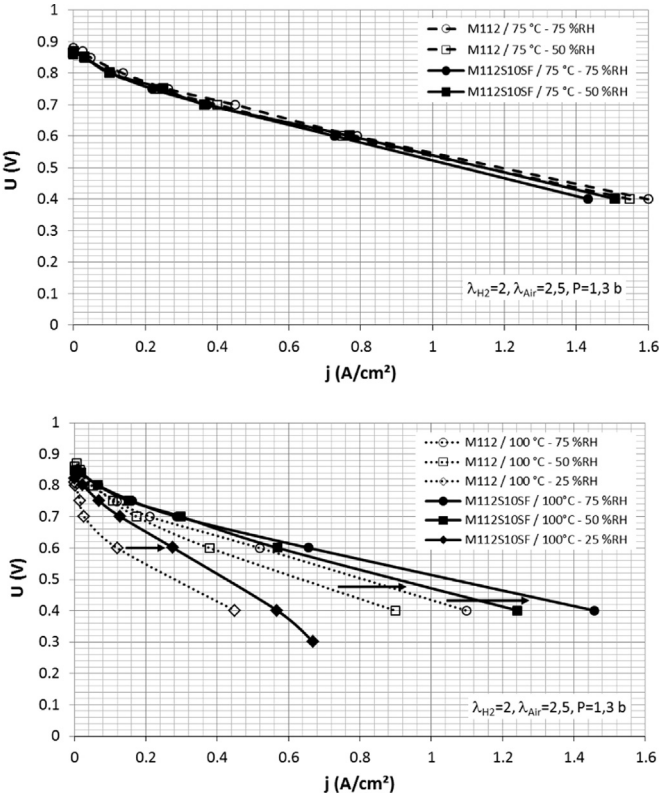



**Fig. 13.** Polarization curves obtained at 75 °C (up) and 100 °C (down) between 25% and 75% relative humidity for M112 (dotted lines) and M112S10SF (solid lines).

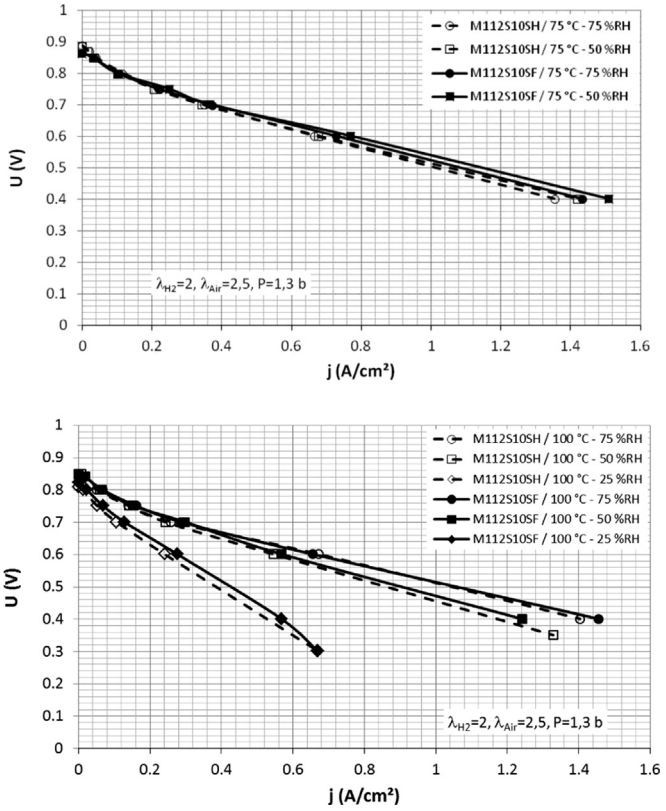



**Fig. 14.** Polarization curves obtained at 75 °C (up) and 100 °C (down) between 25% and 75% relative humidity for M112S10SH (dashed lines) and M112S10SF (solid lines).

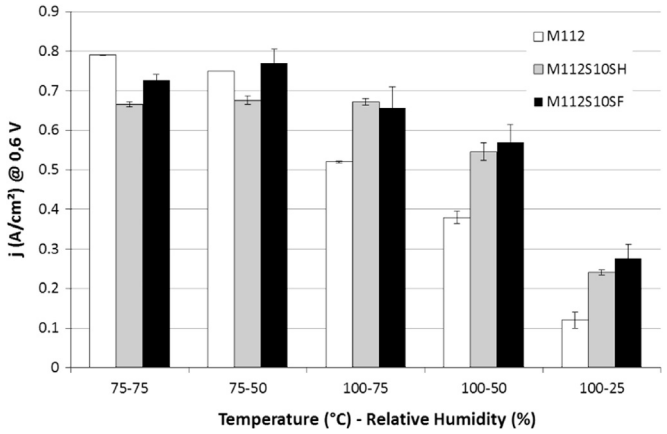



**Fig. 15.** Influence of the temperature and the relative humidity (RH) on the current density at 0.6 V for the different membranes: from left to right M112 (white), M112S10SH (gray), and M112S10SF (black).

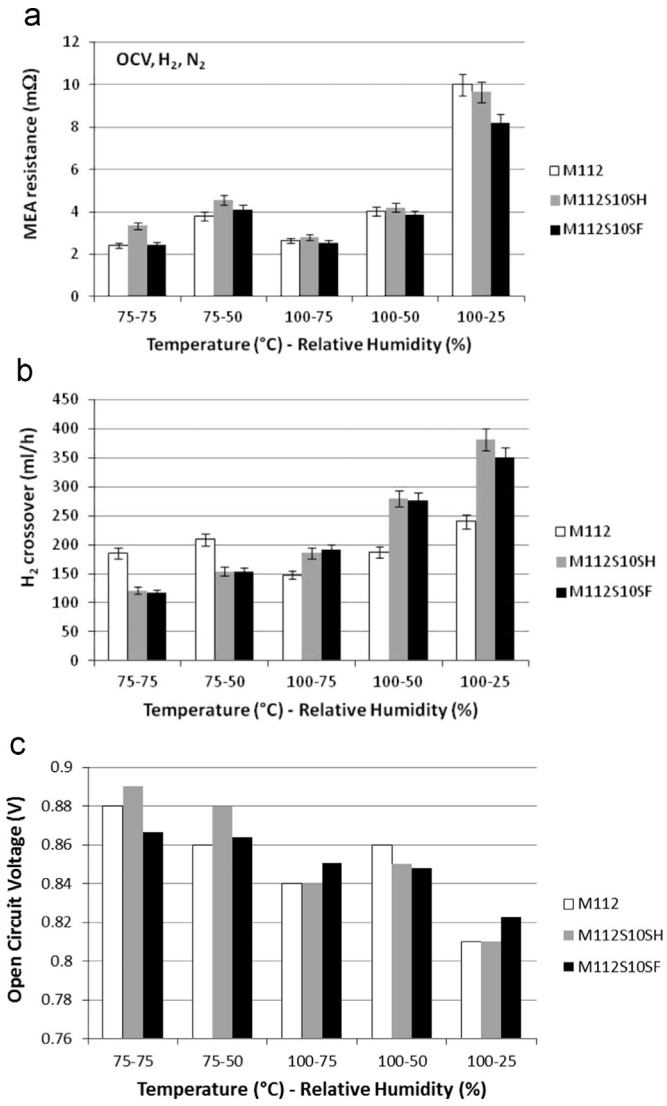



**Fig. 16.** Influence of the temperature and the relative humidity (RH) on the MEA resistance (a), on the $H_2$ crossover (b) and on the open circuit voltage (c), for the different membranes: from left to right M112 (white), M112S10SH (gray), and M112S10SF (black).

our newly modified sepiolite, partly accounting for the better fuel cell performance observed.

Except in severe conditions (100 °C and 25%RH) the hydrogen crossover is similar whatever the type of modified sepiolite added in Nafion®. For both types of membranes, whatever the temperature, the hydrogen crossover is increasing when the relative humidity is decreasing. Regarding the influence of the temperature, we observed two distinct behavior for the pure Nafion® membrane on the one hand and composite membranes on the other hand. Whereas the hydrogen crossover is increasing with the temperature for the composite membranes, keeping the same relative humidity, it is decreasing for the pure Nafion® membrane. We assumed that the dual nature, hydrophobic and hydrophilic, of our newly modified sepiolite was responsible for the improvement of the composite membrane mechanical resistance. The purpose of this modification was to increase the affinity with Nafion® so as to improve the mechanical properties on the one hand and to decrease its gas permeability on the second hand. Indeed we noticed a significant increase of hydrogen crossover with our previously developed composite membranes based on Nafion® and sulfonated sepiolite (M112SxSH series) [59]. Since an increase of hydrogen crossover results in a decrease of open circuit voltage, its limitation is essential. The improvement observed with the newly modified sepiolite is however rather small (Cf Fig. 16b). The only noticeable one was observed at 100 °C and 25%RH. It is however noteworthy that, conjugated with a smaller MEA resistance, it resulted in better fuel cell output power.

Under severe conditions (essentially high temperature), the hydrogen crossover of the new composite membranes is still larger than that of our pure Nafion® cast membrane. We came to the conclusion that the modification performed on sepiolite still need to be improved to decrease the hydrogen crossover. The sepiolite dispersion may indeed still not be optimal as evidenced by TEM observation (Fig. 9).

## 4. Conclusion

The double functionality added to sepiolite revealed to be beneficial to fuel cell performance. Compared to pure Nafion® cast membrane, the composite membranes prepared with this new modified sepiolite allowed improving both the mechanical resistance of the membrane and the fuel cell performance in severe conditions. The elastic modulus was doubled for 10 wt% added sepiolite and 50% more output power at 0.6 V was recorded at 100 °C and 50%RH. The performance are even slightly better than those of our previously developed composite membrane prepared with sulfonated only sepiolite (+4% and +15% more output power at 0.6 V, 100 °C, respectively at 50%RH and 25%RH).

The still large hydrogen crossover suggests that there is still room for improving the affinity between Nafion® and the modified sepiolite. An option would be to play with the size of the functional group so as to impact the internal morphology of the membrane and to optimize the phase segregation within the composite. Finally, long time testing have to be performed to assess the stability of this new composite membrane.

## Acknowledgments

The authors wish to thank the Carnot M.I.N.E.S Institute and Nanomines for financing this study (CARNOT 92822) and TOLSA SA for having provided sepiolite S9 and valuable technical data. They are also grateful to Patrick Leroux (PERSEE), Pierre Ilbizian (PERSEE) and Suzanne JACOMET (CEMEF) for technical support.

## References


[1] A. Chandan, M. Hattenberger, A. El-kharouf, S. Du, A. Dhir, V. Self, B.G. Pollet, A. Ingrama, W. Bujalski, High temperature (HT) polymer electrolyte membrane fuel cells (PEMFC) – a review, J. Power Sources 231 (2013) 264–278.

[2] A.C. Dupuis, Proton exchange membranes for fuel cells operated at medium temperatures: materials and experimental techniques, Prog. Mater. Sci. 56 (3) (2011) 289–327.

[3] P. Staiti, M. Minutoli, S. Hocevar, Membranes based on phosphotungstic acid and polybenzimidazole for fuel cell application, J. Power Sources 90 (2) (2000) 231–235.

[4] J. Peron, E. Ruiz, D.J. Jones, J. Rozières, Solution sulfonation of a novel polybenzimidazole. A proton electrolyte for fuel cell application, J. Membr. Sci. 314 (1–2) (2008) 247–256.

[5] D.J. Jones, J. Roziere, Recent advances in the functionalisation of polybenzimidazole and polyetherketone for fuel cell applications, J. Membr. Sci. 185 (1) (2001) 41–58.

[6] H.L. Lin, Y.C. Chou, T.L. Yu, S.W. Lai, Poly(benzimidazole)-epoxide crosslink membranes for high temperature proton exchange membrane fuel cells, Int. J. Hydrogen Energy 37 (1) (2012) 383–392.

[7] S. Wang, G. Zhang, M. Han, H. Li, Y. Zhang, J. Ni, W. Ma, M. Li, J. Wang, Z. Liu, L. Zhang, H. Na, Novel epoxy-based cross-linked polybenzimidazole for high temperature proton exchange membrane fuel cells, Int. J. Hydrogen Energy 36 (14) (2011) 8412–8421.

[8] D. Aili, Q. Li, E. Christensen, J.O. Jensen, N.J. Bjerrum, Crosslinking of polybenzimidazole membranes by divinylsulfone post-treatment for high-temperature proton exchange membrane fuel cell applications, Polym. Int. 60 (8) (2011) 1201–1207.

[9] J.A. Mader, B.C. Benicewicz, Synthesis and properties of segmented block copolymers of functionalised polybenzimidazoles for high-temperature PEM fuel cells, Fuel Cells 11 (2) (2011) 222–237.

[10] J.A. Mader, B.C. Benicewicz, Sulfonated polybenzimidazoles for high temperature PEM fuel cells, Macromolecules 43 (16) (2010) 6706–6715.

[11] C.H. Park, C.H. Lee, M.D. Guiver, Y.M. Lee, Sulfonated hydrocarbon membranes for medium-temperature and low-humidity proton exchange membrane fuel cells (PEMFCs), Prog. Polym. Sci. 36 (11) (2011) 1443–1498.

[12] A. Stassi, I. Gatto, E. Passalacqua, V. Antonucci, A.S. Arico, L. Merlo, C. Oldani, E. Pagano, Performance comparison of long and short-side chain perfluorosulfonic membranes for high temperature polymer electrolyte membrane fuel cell operation, J. Power Sources 196 (2011) 8925–8930.

[13] Z. Tu, H. Zhang, Z. Luo, J. Liu, Z. Wan, M. Pan, Evaluation of 5 kW proton exchange membrane fuel cell stack operated at 95 °C under ambient pressure, J. Power Sources 222 (2013) 277–281.

[14] A. Ghielmi, P. Vaccarono, C. Troglia, V. Arcella, Proton exchange membranes based on the short-side-chain perfluorinated ionomer, J. Power Sources 145 (2) (2005) 108–115.

[15] K.D. Kreuer, M. Schuster, B. Obliers, O. Diat, U. Traub, A. Fuchs, U. Klock, S. J. Paddison, J. Maier, Short-side-chain proton conducting perfluorosulfonic acid ionomers: why they perform better in PEM fuel cells, J. Power Sources 178 (2) (2008) 499–509.

[16] P.L. Antonucci, A.S. Arico, P. Creti, E. Ramunni, V. Antonucci, Investigation of a direct methanol fuel cell based on a composite Nafion®-silica electrolyte for high temperature operation, Solid State Ion. 125 (1–4) (1999) 431–437.

[17] K.T. Adjemian, S.J. Lee, S. Srinivasan, J. Benziger, A.B. Bocarsly, Silicon oxide Nafion composite membranes for proton-exchange membrane fuel cell operation at 80–140 °C, J. Electrochem. Soc. 149 (3) (2002) A256–A261.

[18] N. Miyake, J.S. Wainright, R.F. Savinell, Evaluation of a sol–gel derived Nafion/silica hybrid membrane for polymer electrolyte membrane fuel cell applications-II. Methanol uptake and methanol permeability, J. Electrochem. Soc. 148 (8) (2001) A905–A909.

[19] T. Ossiander, C. Heinzl, S. Gleich, F. Schönberger, P. Völk, M. Welsch, C. Scheu, Influence of the size and shape of silica nanoparticles on the properties and degradation of a PBI-based high temperature polymer electrolyte membrane, J. Membr. Sci. 454 (2014) 12–19.

[20] Y. Zhao, H. Yang, H. Wu, Z. Jiang, Enhanced proton conductivity of the hybrid membranes by regulating the proton conducting groups anchored on the mesoporous silica, J. Power Sources 270 (2014) 292–303.

[21] Y. Zhao, H. Yang, H. Wu, Z. Jiang, Enhanced proton conductivity of hybrid membranes by incorporating phosphorylated hollow mesoporous silica submicrospheres, J. Membr. Sci. 469 (2014) 418–427.

[22] A.S. Aricò, P. Cretì, P.L. Antonucci, V. Antonucci, Comparison of ethanol and methanol oxidation in a liquid-feed solid polymer electrolyte fuel cell at high temperature, Electrochem. Solid-State Lett. 1 (2) (1998) 66–68.

[23] K.A. Mauritz, Organic–inorganic hybrid materials: perfluorinated ionomers as sol–gel polymerization templates for inorganic alkoxides, Mater. Sci. Eng. C-Biomim. Supramol. Syst. 6 (2–3) (1998) 121–133.

[24] Gh Mohammadi, M. Jahanshahi, A. Rahimpour, Fabrication and evaluation of Nafion nanocomposite membrane based on $ZrO_2$–$TiO_2$ binary nanoparticles as fuel cell MEA, Int. J Hydrogen Energy 8 (22) (2013) 9387–9394.

[25] K. Ketpang, B. Son, D. Lee, S. Shanmugam, Porous zirconium oxide nanotube modified Nafion composite membrane for polymer electrolyte membrane fuel cells operated under dry conditions, J. Membr. Sci. 488 (2015) 154–165.

[26] M. Watanabe, H. Uchida, Y. Seki, M. Emori, P. Stonehart, Self-humidifying polymer electrolyte membranes for fuel cells, J. Electrochem. Soc. 143 (12) (1996) 3847–3852.

[27] A. Sacca, A. Carbone, E. Passalacqua, A. D'Epifanio, E. Traversa, E. Sala, F. Traini, R. Ornelas, Nafion-$TiO_2$ hybrid membranes for medium temperature polymer electrolyte fuel cells (PEFCs), J. Power Souces 152 (1) (2005) 16–21.

[28] V. Di Noto, M. Bettiol, F. Bassetto, N. Boaretto, E. Negro, S. Lavina, F. Bertasi, Hybrid inorganic–organic nanocomposite polymer electrolytes based on Nafion and fluorinated $TiO_2$ for PEMFCs, Int. J. Hydrogen Energy 37 (7) (2012) 6169–6181.

[29] Y. Yin, T. Xu, X. Shen, H. Wu, Z. Jiang, Fabrication of chitosan/zwitterion functionalized titania–silica hybrid membranes with improved proton conductivity, J. Membr. Sci. 469 (2014) 355–363.

[30] H. Wu, Y. Cao, X. Shen, Z. Li, T. Xu, Z. Jiang, Preparation and performance of different amino acids functionalized titania-embedded sulfonated poly (ether ether ketone) hybrid membranes for direct methanol fuel cells, J. Membr. Sci. 463 (2014) 134–144.

[31] K. Hooshyari, M. Javanbakht, L. Naji, Morteza Enhessari, nanocomposite proton exchange membranes based on Nafion containing $Fe_2TiO_5$ nanoparticles in water and alcohol environments for PEMFC, J. Membr. Sci. 454 (2014) 74–81.

[32] K. Ketpang, K. Lee, S. Shanmugam, Facile synthesis of porous metal oxide nanotubes and modified nafion composite membranes for polymer electrolyte fuel cells operated under low relative humidity, ACS Appl. Mater. Interfaces 6 (2014) 16734–16744.

[33] E. Peled, T. Duvdevani, A. Melman, A novel proton-conducting membrane, Electrochem. Solid State Lett. 1 (5) (1998) 210–211.

[34] P. Staiti, A.S. Aricò, V. Baglio, F. Lufrano, E. Passalacqua, V. Antonucci, Hybrid Nafion-silica membranes doped with heteropolyacids for application in direct methanol fuel cells, Solid State Ion. 145 (2001) 101–107.

[35] Z.G. Shao, H. Xu, M.Q. Li, I.M. Hsing, Hybrid Nafion-inorganic oxides membrane doped with heteropolyacids for high temperature operation of proton exchange membrane fuel cell, Solid State Ion. 177 (2006) 779–785.

[36] M. Helen, B. Viswanathan, S. Srinivasa Murthy, Synthesis and characterization of composite membranes based on alpha-zirconium phosphate and silicotungstic acid, J. Membr. Sci. 292 (1–2) (2007) 98–105.

[37] S. Shanmugam, B. Viswanathan, T.K. Varadarajan, Synthesis and characterization of silicotungstic acid based organic-inorganic nanocomposite membrane, J. Membr. Sci. 275 (1–2) (2006) 105–109.

[38] J.L. Lu, Q.H. Fang, S.L. Li, S.P. Jiang, A novel phosphotungstic acid impregnated meso-Nafion multilayer membrane for proton exchange membrane fuel cells, J. Membr. Sci. 427 (2013) 101–107.

[39] G. Alberti, M. Casciola, R. Palombari, Inorgano–organic proton conducting membranes for fuel cells and sensors at medium temperatures, J. Membr. Sci. 172 (1–2) (2000) 233–239.

[40] G. Alberti, M. Casciola, D. Capitani, A. Donnadio, R. Narducci, M. Pica, M. Sganappa, Novel Nafion-zirconium phosphate nanocomposite membranes with enhanced stability of proton conductivity at medium temperature and high relative humidity, Electrochem. Acta 52 (2007) 8125–8132.

[41] P. Costamagna, C. Yang, A.B. Bocarsly, S. Srinivasan, Nafion® 115/zirconium phosphate composite membranes for operation of PEMFCs above 100 °C, Electrochem. Acta 47 (7) (2002) 1023–1033.

[42] A. Donnadio, M. Pica, D. Capitani, V. Bianchi, M. Casciola, Layered zirconium alkylphosphates: suitable materials for novel PFSA composite membranes with improved proton conductivity and mechanical stability, J. Membr. Sci. 462 (2014) 42–49.

[43] F. Mura, R.F. Silva, A. Pozio, Study on the conductivity of recast Nafion®/montmorillonite and Nafion®/$TiO_2$ composite membranes, Electrochem. Acta 52 (19) (2007) 5824–5828.

[44] Y.F. Lin, C.Y. Yen, C.H. Hung, Y.H. Hsiao, C.C.M. Ma, A novel composite membranes based on sulfonated montmorillonite modified Nafion® for DMFCs, J. Power Sources 168 (1) (2007) 162–166.

[45] D.H. Jung, S.Y. Cho, D.H. Peck, D.R. Shin, J.S. Kim, Preparation and performance of a Nafion®/montmorillonite nanocomposite membrane for direct methanol fuel cell, J. Power Sources 18 (1–2) (2003) 205–211.

[46] R.F. Silva, S. Passerini, A. Pozio, Solution-cast Nafion®/montmorillonite composite membrane with low methanol permeability, Electrochim. Acta 50 (13) (2005) 2639–2645.

[47] J.M. Thomassin, C. Pagnoulle, G. Caldarella, A. Germain, R. Jérôme, Impact of acid containing montmorillonite on the properties of Nafion® membranes, Polymer 46 (25) (2005) 11389–11395.

[48] J.M. Thomassin, C. Pagnoulle, D. Bizzari, G. Caldarella, A. Germain, R. Jérôme, Improvement of the barrier properties of Nafion® by fluoro-modified montmorillonite, Solid State Ion. 177 (13–14) (2006) 1137–1144.

[49] P. Bebin, M. Caravanier, H. Galiano, Nafion®/clay-$SO_3H$ membrane for proton exchange membrane fuel cell application, J. Membr. Sci. 278 (1–2) (2006) 35–42.

[50] J.H. Chang, J.H. Park, G.G. Park, C.S. Kim, O.O. Park, Proton-conducting composite membranes derived from sulfonated hydrocarbon and inorganic materials, J. Power Sources 124 (1) (2003) 18–25.

[51] I. Nicotera, A. Enotiadis, K. Angjeli, L. Coppola, D. Gournis, Evaluation of smectite clays as nanofillers for the synthesis of nanocomposite polymer electrolytes for fuel cell applications, Int. J. Hydrogen Energy 37 (7) (2012) 6236–6245.

[52] C. Lixon Buquet, K. Fatyeyeva, F. Poncin-Epaillard, P. Schaetzel, E. Dargent, D. Langevin, Q.T. Nguyen, S. Marais, New hybrid membranes for fuel cells: Plasma treated laponite based sulfonated polysulfone, J. Membr. Sci. 351 (1–2) (2010) 1–10.

[53] C.S. Karthikeyan, S.P. Nunes, L.A.S.A. Prado, M.L. Ponce, H. Silva, B. Ruffmann, K. Schulte, Polymer nanocomposite membranes for DMFC application, J.

Membr. Sci. 254 (1–2) (2005) 139–146.
[54] F. Xu, S. Mu, M. Pan, Mineral nanofibre reinforced composite polymer electrolyte membranes with enhanced water retention capability in PEM fuel cells, J. Membr. Sci. 377 (2011) 134–140.
[55] F. Xu, R. Xu, S. Mu, Nano mineral fiber enhanced catalyst coated membranes for improving polymer electrolyte membrane fuel cell durability, J. Power Sources 196 (24) (2011) 10563–10569.
[56] F.J. Fernandez-Carretero, V. Compañ, E. Riande, Hybrid ion-exchange membranes for fuel cells and separation processes, J. Power Sources 173 (1) (2007) 68–76.
[57] F.J. Fernandez-Carretero, E. Riande, C. del Rio, F. Sanchez, J.L. Acosta, V. Compañ, Preparation and characterization of hybrid membranes based on Nafion® using partially sulfonated inorganic fillers, J. New Mater. Electrochem. Syst. 13 (2) (2010) 83–93.
[58] F.J. Fernandez-Carretero, K. Suarez, O. Solorza, E. Riande, V. Compañ, PEMFC performance of MEAS based on Nafion® and sPSEBS hybrid membranes, J. New Mater. Electrochem. Syst. 13 (3) (2010) 191–199.
[59] C. Beauger, G. Lainé, A. Burr, A. Taguet, B. Otazaghine, A. Rigacci, Nafion®-sepiolite composite membranes for improved proton exchange membrane fuel cell performance, J. Membr. Sci. 430 (2013) 167–179.
[60] M.E. Mackay, A. Tuteja, P.M. Duxbury, C.J. Hawker, B. Van Horn, Z. Guan, G. Chen, R.S. Krishnan, General strategies for nanoparticle dispersion, Science 311 (2006) 1740–1743.
[61] R. Krishnamoorti, Strategies for dispersing nanoparticles in polymers, MRS bull. 32 (2007) 341–347.
[62] G. Fleer, Polymers at interfaces and in colloidal dispersions, Adv. Colloid Interface Sci. 159 (2010) 99–116.
[63] Y. Lipatov, Polymer blends and interpenetrating polymer networks at the interface with solids, Prog. Polym. Sci. 27 (2002) 1721–1801.
[64] E. Glogowski, R. Tangirala, Functionalization of nanoparticles for dispersion in polymers and assembly in fluids, J. Polym. Sci. A: Polym. Chem. 44 (2006) 5076–5086.
[65] N. Fukaya, H. Haga, T. Tsuchimoto, Organic functionalization of the surface of silica with arylsilanes. A new method for synthesizing organic–inorganic hybrid materials, J. Organomet. Chem. 695 (2010) 2540–2542.
[66] M. Lazghab, K. Saleh, P. Guigon, Functionalisation of porous silica powders in a fluidised-bed reactor with glycidoxypropyltrimethoxysilane (GPTMS) and aminopropyltriethoxysilane (APTES), Chem. Eng. Res. Des. 88 (2010) 686–692.
[67] M. Luechinger, R. Prins, G. Pirngruber, Functionalization of silica surfaces with mixtures of 3-aminopropyl and methyl groups, Microporous Mesoporous Mater. 85 (2005) 111–118.
[68] N. García, J. Guzmán, E. Benito, A. Esteban-Cubillo, E. Aguilar, J. Santarén, P. Tiemblo, Surface modification of sepiolite in aqueous gels by using methoxysilanes and its impact on the nanofiber dispersion ability, Langmuir 27 (2011) 3952–3959.
[69] C. Vestal, Z. Zhang, Atom transfer radical polymerization synthesis and magnetic characterization of $MnFe_2O_4$/polystyrene core/shell nanoparticles, J. Am. Chem. Soc. 124 (2002) 14312–14313.
[70] T. Wang, C. Ou, C. Yang, Synthesis and properties of organic/inorganic hybrid nanoparticles prepared using atom transfer radical polymerization, J. Appl. Polym. Sci. 109 (2008) 3421–3430.
[71] M. Ouattara-Brigaudet, C. Beauger, S. Berthon-Fabry, P. Achard, Carbon aerogels as catalyst supports and first insights on their durability in proton exchange membrane fuel cells, Fuel Cells 11 (6) (2011) 726–734.
[72] W. Vielstich, A. Lamm, H. Gasteiger, Principles of MEA preparation, Handbook of Fuel Cells – Fundamentals, Technology and Applications, Wiley, Chichester, UK (2003), p. 538.
[73] K.T. Adjemian, R. Dominey, L. Krishnan, H. Ota, P. Majsztrik, T. Zhang, J. Mann, B. Kirby, L. Gatto, M. Velo-Simpson, J. Leahy, S. Srinivasan, J.B. Benziger, A. B. Bocarsly, Function and characterization of metal oxide – Nafion composite membranes for elevated-temperature $H_2/O_2$ PEM fuel cells, Chem. Mater. 18 (9) (2006) 2238–2248.